JOURNAL OF AGRICULTURAL AND FOOD CHEMISTRY

Champagne Experiences Various Rhythmical Bubbling Regimes in a Flute

GÉRARD LIGER-BELAIR,*,† ALBERTO TUFAILE,§ PHILIPPE JEANDET,† AND JOSÉ-CARLOS SARTORELLI§

Laboratoire d'Œnologie et Chimie Appliquée, UPRES EA 2069, URVVC, Faculté des Sciences de Reims, B.P. 1039, 51687 Reims Cedex 2, France, and Instituto de Física, Universidade de São Paulo, Caixa Postal 66318, 05315-970 São Paulo, SP, Brazil

Bubble trains are seen rising gracefully from a few points on the glass wall (called nucleation sites) whenever champagne is poured into a glass. As time passes during the gas-discharging process, the careful observation of some given bubble columns reveals that the interbubble distance may change suddenly, thus revealing different rhythmical bubbling regimes. Here, it is reported that the transitions between the different bubbling regimes of some nucleation sites during gas discharging is a process which may be ruled by a strong interaction between tiny gas pockets trapped inside the nucleation site and/or also by an interaction between the tiny bubbles just blown from the nucleation site.

KEYWORDS: Champagne; sparkling wines; carbonated beverages; effervescence; bubble nucleation; nucleation sites; bubbling instabilities; cellulose fibers

INTRODUCTION

In champagne and sparkling wines, an excess of carbon dioxide molecules is formed with ethanol when yeasts ferment sugars. They are responsible for producing gas bubbles as soon as the bottle is uncorked. In soda drinks and most fizzy waters, industrial carbonation is the source of effervescence (*1*).

In weakly supersaturated liquids such as carbonated beverages in general, bubble formation and growth require preexisting gas cavities with radii of curvature large enough to overcome the nucleation energy barrier and grow freely (*2*, *3*). Closer inspection of glasses poured with champagne revealed that most of the bubble nucleation sites were found to be located on preexisting gas cavities trapped inside hollow and roughly cylindrical cellulose-fiber-made structures on the order of 100 μm long with a cavity mouth of several micrometers (*4*−*6*). These fibers are released from the surrounding air or from the towel used to wipe the glass. Fibers probably adhere on the flute wall due to electrostatic forces (especially if the glass or flute is vigorously wiped by a towel). Flutes that have been cleaned with a towel before use show an excess of bubble nucleation sites and, therefore, an excess of effervescence (*7*). Therefore, there is a substantial variation between flutes depending on how the flute was cleaned and how it was left before serving. If it is not wiped by use of a towel and left upside down during the drying process, fibers will not be able to settle and adhere on the glass wall, for example.

* Corresponding author [telephone 00 (33)3 26 91 86 14; fax 00 (33)3 26 91 33 40; e-mail gerard.liger-belair@univ-reims.fr].
† Faculté des Sciences de Reims.
§ Universidade de São Paulo.

It is also well-known that bubbles may also arise from microscratches on the glass wall (*8*, *9*), done intentionally by the glassmaker to produce effervescence. A rendering of such microscratches done by a glassmaker at the bottom of a champagne flute is displayed in **Figure 1**. However, in a glass without such a specific treatment, irregularities of the glass itself are unable to entrap gas cavities of a critical size needed to produce bubble formation. In this paper we nevertheless exclusively focused on bubbling from cellulose fibers, which are the most common source of bubbles in carbonated beverages.

The hollow cavity inside these fibers where the gas pocket is trapped during the pouring process is called the lumen. The mechanism of bubble release from a fiber's lumen has already been described and partly modeled in recent papers (*4*−*6*, *10*). In short, after the opening of a bottle of champagne or sparkling wine, the thermodynamic equilibrium of CO_2 molecules dissolved in the liquid medium is broken. The dissolved CO_2 molecules become in excess compared to what the liquid medium can hold. Therefore, CO_2 molecules will escape from the liquid medium through every available gas/liquid interface to reach a vapor phase. Actually, once the sparkling beverage is poured into a glass, the tiny gas pockets trapped inside the collection of fibers adsorbed on the glass wall offer gas/liquid interfaces to the dissolved CO_2 molecules, which cross the interface toward the gas pockets. In turn, gas pockets grow inside the fibers' lumen. When a gas pocket reaches the tip of a fiber, a bubble is ejected, but a portion of the gas pocket remains trapped inside the fiber's lumen and shrinks back to its initial position, and the cycle starts again until bubble production stops through lack of dissolved gas molecules (cf. **Figure 2**). The fiber displayed in **Figure 2** is a sort of textbook case, the

10.1021/jf061250n CCC: $33.50
Published on Web 08/26/2006

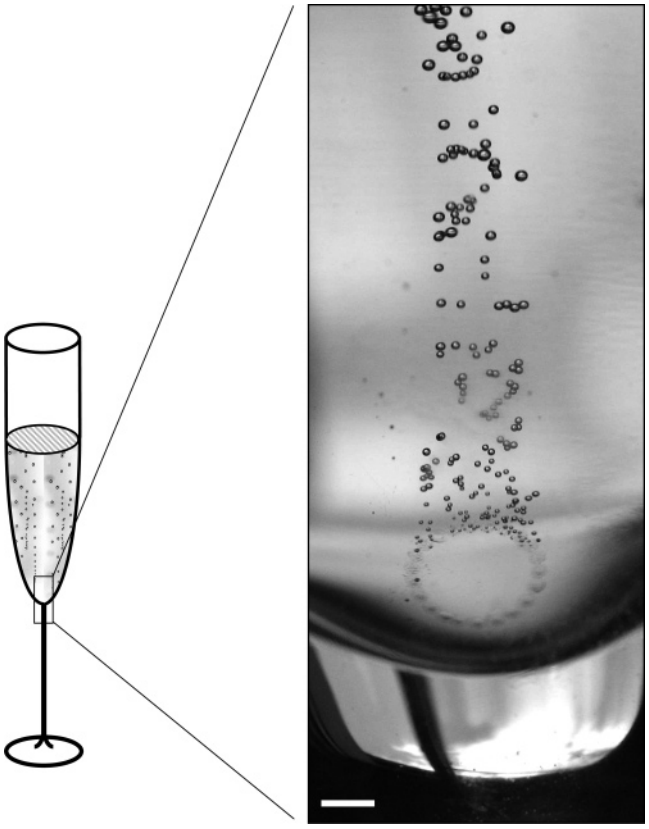

Figure 1. At the bottom of this flute, the glassmaker has engraved a small ring. Bubbles are seen generated from these "artificial" microscratches. Bar = 1 mm.

behavior of which was recently understood and modeled (*10*). Studies of the fine mechanisms behind the regular production of bubbles from those tiny hollow and cylindrical structures are indeed still in progress (*11*).

Actually, the process mentioned above and illustrated in **Figure 2** basically describes the repetitive and clockwork bubble production, but this clockwork process may sometimes be suddenly broken at some given nucleation sites, which show a much more intriguing way of blowing bubbles during the gas-discharging process. In a previous paper, we have already reported that the bubbling transitions of some nucleation sites undergo a sequence known as the "period-adding" route, based on a model that takes into account the coupling between the bubbling frequency and the frequency of the gas pocket, which oscillates while trapped inside the fiber's lumen (*12*). However, numerous bubble nucleation sites found on the wall of a glass poured with champagne, sparkling wine, or soda and showing bubbling instabilities as time proceeds do not fit the period-adding scenario.

The aim of this work, based on close observation of some other nucleation sites presenting sequences of bubbling instabilities during gas discharging in a flute, is twofold: (i) to underscore and describe the phenomenon of bubbling transitions as time progresses during the gas discharge; and (ii) to propose that the transitions between the successive bubbling regimes could also be ruled by an interaction between multiple gas pockets trapped inside the fiber's lumen and/or by an interaction between the tiny bubbles just blown from the fiber's tip.

MATERIALS AND METHODS

The close observation of nucleation sites was conducted in situ, at room temperature (20 ± 2 °C), in a classic crystal flute (Marianna, Lednické, Slovakia) with a diameter of 4.9 cm and a wall thickness of 0.8 mm poured with a standard commercial Champagne wine (supplied by Champagne Pommery, Reims, France). A sample of 150 mL of champagne was poured into the flute, which was first rinsed using distilled water and then air-dried. To avoid the effect of the initial liquid convection on bubble formation, nucleation sites were observed at least 3 min after the champagne had been poured into the flute.

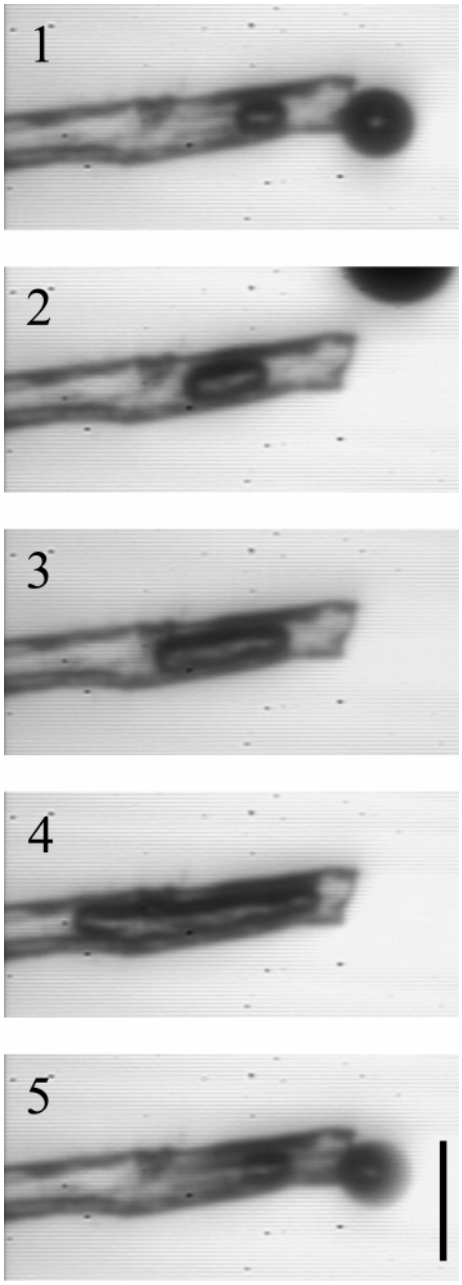

Figure 2. Time sequence illustrating one period of the cycle of bubble birth from the lumen of a typical hollow cellulose fiber adsorbed on the wall of a glass poured with champagne; the time interval between successive frames is ≈200 ms. Bar = 50 μm. Reprinted with permission from ref *10*. Copyright 2005 American Chemical Society.

Close-up photographs of bubble trains experiencing bubbling transitions were taken with a photographic camera (Olympus OM2) fitted with bellows and with a 50:1.8 objective. Close observation of the nucleation sites themselves was conducted using a high-speed digital video camera (Speedcam+, Vannier Photelec, France) capable of 2000 frames per second and which was fitted with a microscope objective (M Plan Apo 5, Mitutoyo, Japan). The time resolution of our high-speed camera enabled us to examine details of the bubble production process. The flute was placed on a micrometric plate, which enabled a

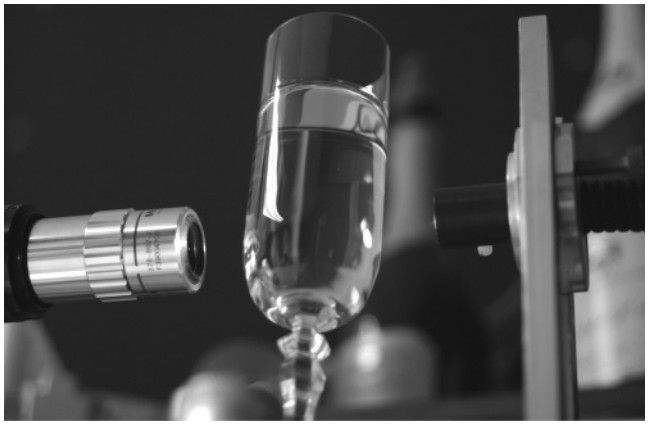

Figure 3. Photographic detail of the workbench used to observe bubble nucleation sites in close-up.

precise rotation of the flute in front of the objective. A cold back-light was placed behind the flute. To homogenize the light, a white translucent plastic screen was placed between the flute and the back-light. To have access to the dynamics of bubbling from nucleation sites, the microscope objective was pointed at the base of each bubble train investigated. A photographic detail of the microscope objective pointing to a nucleation site is displayed in **Figure 3**.

RESULTS AND DISCUSSION

After the champagne had been poured into the flute, thorough examination (even by the naked eye) of the bubble trains rising toward the liquid surface revealed a curious and quite unexpected phenomenon. As time proceeds, during the gas-discharging process from the liquid matrix, some of the bubble trains showed abrupt transitions during the repetitive and rhythmical production of bubbles. Visually speaking, the macroscopic pertinent parameter that is characteristic from the successive bubbling regimes is the interbubble distance between the successive bubbles of a given bubble train. **Figure 4** illustrates the sudden changes in the bubbling regimes from a given nucleation site producing bubbles at the bottom of the flute. In **Figure 4**, micrographs of a bubble train in its successive rhythmical bubbling regimes while degassing are displayed. The duration of a given bubbling regime may vary from a few seconds to several minutes. In frame **a**, bubbles are seen to be generated from a period-2 bubbling regime, which is characterized by the fact that two successive bubbles rise in pairs. Then, the bubbling regime suddenly changes, and a multiperiodic bubbling regime arises, which is displayed in frame **b**. Later, in frame **c**, a clockwork bubbling in period 1 occurs when the distance between two successive bubbles increases monotonically as they rise, and so on. This nucleation site experienced various other bubbling regimes during its life, until it finally ended in a clockwork period-1 bubbling regime presented in frame **g**.

To clearly identify the succession of the numerous bubbling regimes experienced by nucleation sites during the degassing process, the time intervals between the successive bubbles blown from various nucleation sites were measured as time proceeds, in situ, by high-speed video recordings. For each given nucleation site, time series were obtained that show the

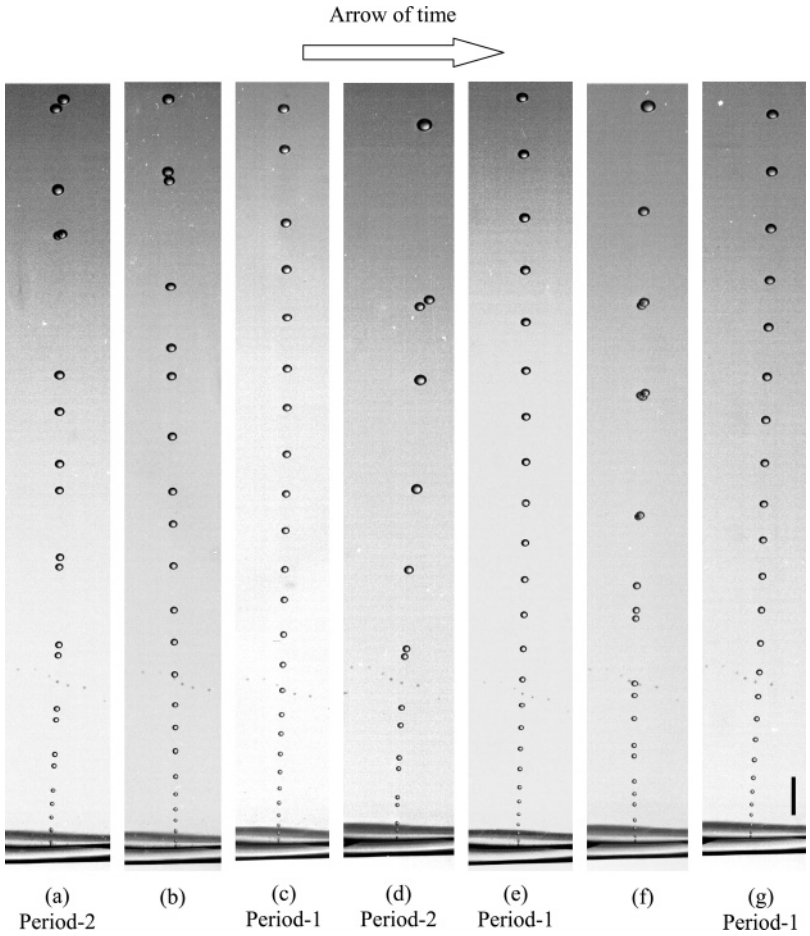

Figure 4. Time sequence (from left to right) showing a bubble nucleation site at the bottom of a flute poured with champagne blowing bubbles through different and well-established bubbling regimes. Bar = 1 mm.

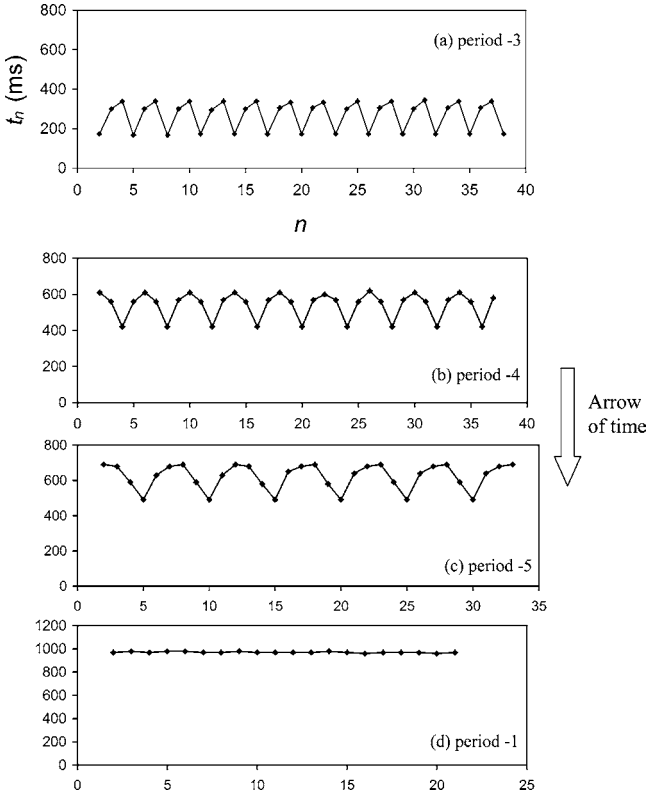

Figure 5. Four time series showing the time interval t_n between the successive bubbles blown from a fiber's tip showing four well-established bubbling regimes during the gas discharging process (n is the index assigned to a bubble in the bubble train).

successive time intervals t between the successive bubbles, that is, t_1, t_2, t_3, ..., t_{n-1}, t_n, t_{n+1}, ..., n being the index assigned to the nth bubble of the bubble train. From the single time series thus obtained, a simple analytical method was then used to visualize the rhythmicity in the production of bubbles from a nucleation site (*13*). The time intervals between successive bubbles were simply plotted as a function of one another (i.e., t_{n+1} versus t_n). The obtained graph is called the return map. If the return map corresponding to a given time series contains a single dot-cloud only, the nucleation site is in a period-1 bubbling regime, that is, bubbles are released monotonously with a constant time interval between each bubble. Currently, due to sudden transitions between successive bubbling regimes, it is possible that more dot-clouds show up in the map. Generally speaking, the nucleation site is multiperiodic and has a periodicity equal to the number of dot-clouds in the corresponding return map.

During degassing, the successive time series of a given nucleation site as well as the corresponding return maps are displayed in **Figures 5** and **6**, respectively. When the average bubbling frequency of the nucleation site is ≈4 bubbles/s, the bubbling occurs in a period-3 regime (see **Figure 6a**). Further decrease of the average bubbling frequency to 2 bubbles/s modifies the bubbling regime, which suddenly turns in a period-4 regime (see **Figure 6b**). When the average bubbling frequency is ≈1.5 bubbles/s, another regime takes place, and the nucleation site blows bubbles in a period-5 regime (see **Figure 6c**). Ultimately, for a bubbling frequency close to 1 bubble/s, the time interval between successive bubbles collapses in a monotonously period-1 behavior (see **Figure 6d**). Thus, it clearly appears that this given nucleation site experienced numerous bubbling regimes during its fleeting life, to finally release bubbles in a clockwork period-1 bubbling regime.

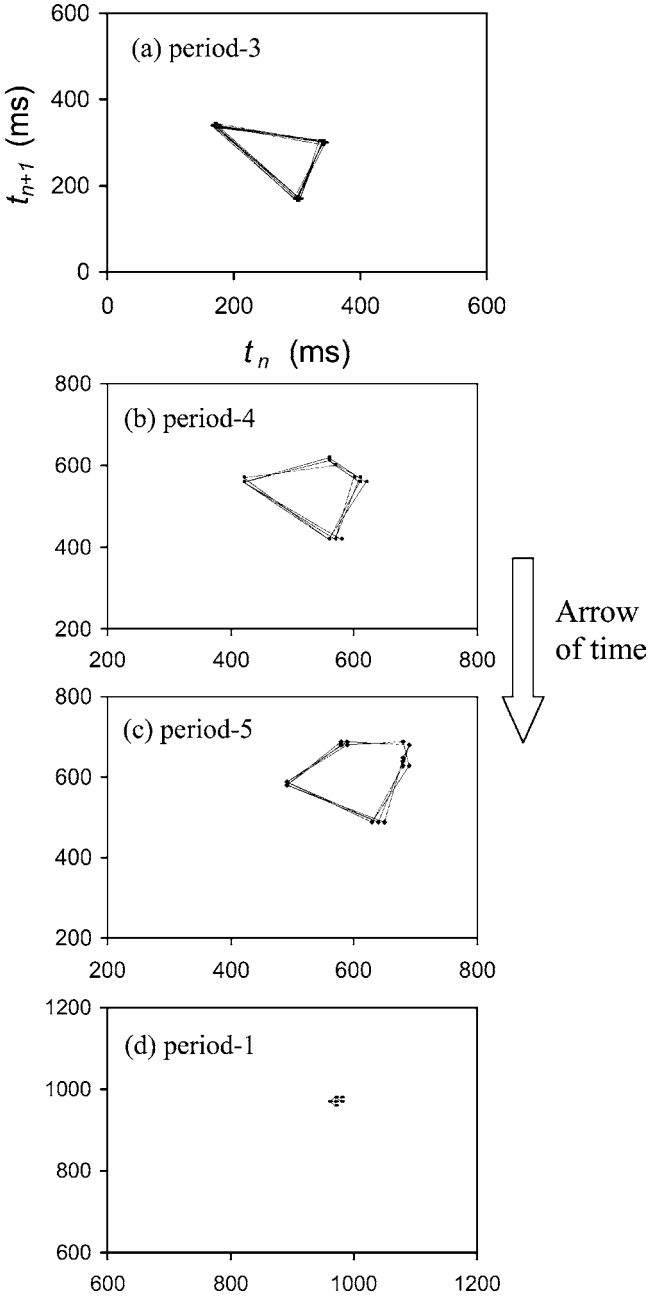

Figure 6. Four return maps corresponding to the four time series presented in **Figure 5**. The periodicity of the bubbling regime is equal to the number of dot-clouds in each map.

Such a curious and unexpected observation raises the following question: what is/are the mechanism(s) responsible for the transitions between the different bubbling regimes?

To better identify the fine mechanisms behind this rhythmical production of bubbles from a few nucleation sites, some of them experiencing bubbling transitions were filmed in situ by use of the high-speed digital video camera. Two time sequences are displayed in **Figures 7** and **8**, where bubbles are blown in a period-2 and in a very erratic way, respectively. The lumen of the cellulose fiber displayed in **Figure 7** shows numerous gas pockets growing, interacting together, and breaking while releasing a bubble at the fiber's tip (see frames **c**, **e**, and **i** of **Figure 7**). This is a crucial difference with the case of the fiber displayed in **Figure 2**, where there is only a single gas pocket that grows inside the lumen, breaks at the end of the fiber tip, and therefore releases a bubble with clockwork regularity (*10*).

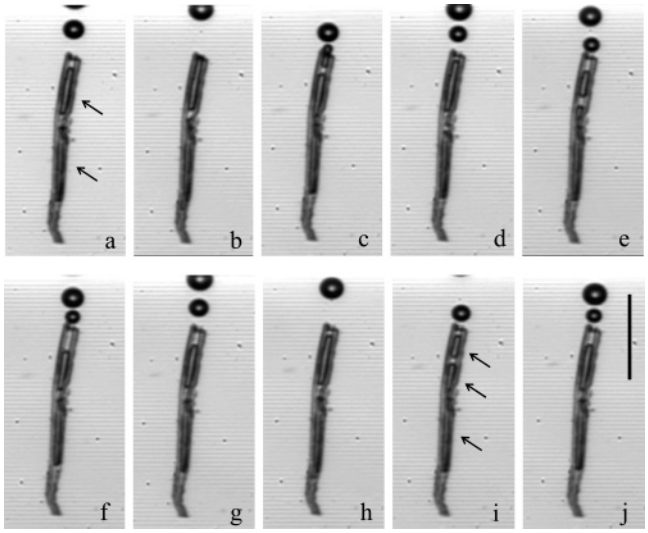

Figure 7. Time sequence showing a cellulose fiber releasing bubbles by pairs, that is, in a period-2 bubbling regime. The black arrows point to the various gas pockets interacting. The time interval between two successive frames is 100 ms. Bar = 100 μm.

The fiber's lumen displayed in **Figure 8**, which is wider than that displayed in **Figure 7**, clearly shows two gas pockets periodically touching and connecting themselves through a tiny gas bridge (see frames **c**, **d**, **f**, and **i** of **Figure 8**). The micrometric gas bridge connecting the two gas pockets and disturbing the overall production of bubbles is enlarged in **Figure 9**. This tiny gas bridge is a likely source of instability in comparison with the classical textbook case of the single gas pocket fiber displayed in **Figure 2** (*10*). Furthermore, it is worth noting that contrary to the fiber displayed in **Figure 7**, where gas pockets could freely move while interacting inside their cylindrical "sleeve" of cellulose, the two gas pockets trapped in the lumen of the fiber displayed in **Figure 8** are fixed. This observation seems to indicate that the wettability of the lumen's inner wall may vary from one fiber to another. The huge diversity of our observations, in terms of the various successive bubbling regimes, is also directly linked with the "natural" variability of cellulose fibers (in terms of size, lumen diameter, inner wall properties, etc.).

In a previous paper, instabilities from a cellulose fiber were already reported (*12*). The previously published data showed a general rule concerning instabilities arising from some fibers presenting just one trapped gas pocket. In our previous paper, the successive rythmical bubbling regimes followed the so-called period-adding scenario (*12*). Nevertheless, this previously published scenario does not fit the various ways of blowing bubbles from more complex cellulose fibers able to entrap numerous gas pockets as shown in **Figures 7** and **8**. Numerous fibers, such as those shown in the present paper, presented a sequence of various bubbling instabilities, which is not reproduced by our previous model (*12*). A huge collection of successive rythmical bubbling regimes has been observed, and the highest recorded periodicity was observed for a fiber presenting a period-12 bubbling regime. The only rule which seems to fit our observations at this step is that the numerous fibers (with one or numerous gas pockets interacting) followed as time progresses seem to always end in a clockwork period-1 bubbling regime. In the future, we plan to modify our previously developed model to add other gas pockets and to force an interaction between them. At the moment, we could not find any general rule with fibers presenting numerous gas pockets interacting together, but the close-up observation and the discovery of the multiple gas pockets interacting together are considered to be a step toward a deeper understanding of the successive rythmical bubbling regimes arising from complex fibers.

During the observation in close-up of the release of bubbles from numerous nucleation sites showing instabilities in their bubbling regimes, another source of instability was underscored, which adds further to the sources of instability described above. The tiny bubbles just blown from the fiber's tip may sometimes coalesce (see **Figure 10**), thus modifying the overall number of bubbles produced from the nucleation site, the allure of the bubble train as seen by the taster, and finally the overall degassing process in the flute.

This paper reports close-up films showing some of the mechanisms behind the bubbling instabilities observed in a flute poured with champagne. The complex interplay between gas pockets trapped inside nucleation sites was found to be the key parameter leading to bubbling instabilities. We also have observed similar bubbling instabilities and transitions in glasses poured with various sparkling wines and soda drinks, where

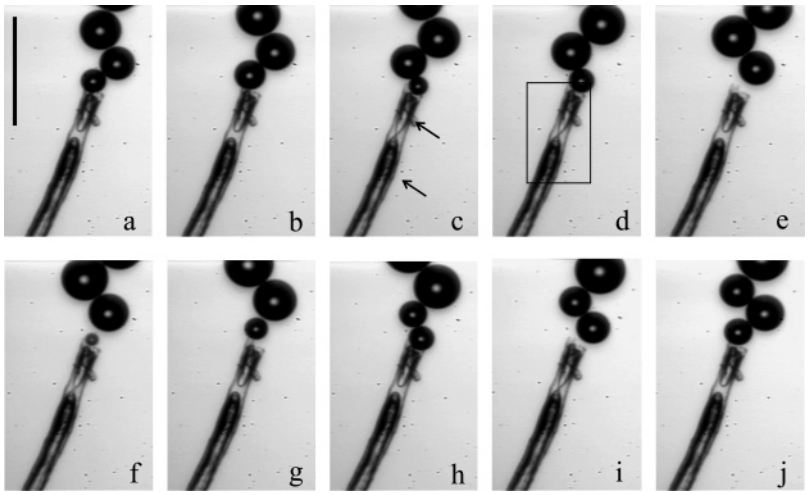

Figure 8. Time sequence showing a cellulose fiber releasing bubbles in a very erratic way, without periodicity, contrary to the fiber displayed in **Figure 7**. Two fixed gas pockets are interacting in the lumen of this cellulose fiber, thus disturbing the periodicity of the bubbling regime. The black arrows point to the various gas pockets interacting. The time interval between two successive frames is 10 ms. Bar = 100 μm.

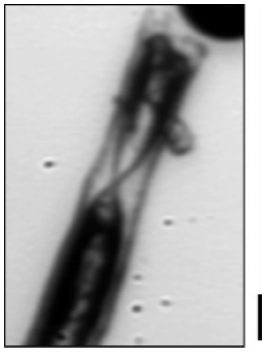

Figure 9. Detail of the cellulose fiber displayed in **Figure 8**, which clearly shows the establishment of a micrometric gas bridge between the two gas pockets trapped inside the fiber's lumen. Bar = 10 μm.

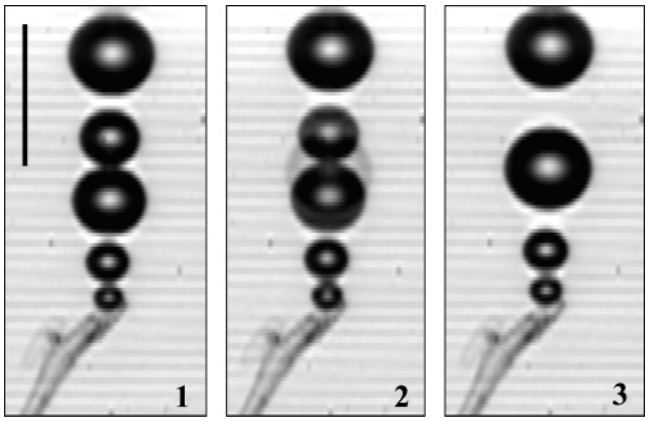

Figure 10. Time sequence showing the coalescence of two bubbles rising in-line. The time interval between two frames is ≈4 ms. In-line coalescence may also be responsible for the breaking between different and well-established bubbling regimes. Bar = 100 μm.

most of bubble nucleation sites were also identified as being cellulose fibers.

Furthermore, bubbling instabilities are observed in a huge quantity of everyday situations, from the food industry (effervescence and foaming) to biological systems (embolism in plants). Even human beings may be concerned by the formation of bubbles. Actually, nitrogen bubbles may arise and grow in the bloodstream of divers who have breathed high-pressure air if they resurface too quickly. These observations conducted in a simple flute poured with champagne may therefore also extend to the more general field of heterogeneous bubble nucleation and could eventually contribute to the unlocking of some of the mysteries hidden behind bubble formation from gas cavities.

ACKNOWLEDGMENT

Thanks are due to Champagne Möet & Chandon and Pommery for supplying wines and to Arc International for supporting our research.

LITERATURE CITED

(1) Liger-Belair, G. *Uncorked: The Science of Champagne*; Princeton University Press: Princeton: NJ, 2004.
(2) Jones, S. F.; Evans, G. M.; Galvin, K. P. Bubble nucleation from gas cavities: a review. *Adv. Colloid Interface Sci.* **1999**, *80*, 27−50.
(3) Lubetkin, S. D. Why is it much easier to nucleate gas bubbles than theory predicts? *Langmuir* **2003**, *19*, 2575−2587.
(4) Liger-Belair, G.; Vignes-Adler, M.; Voisin, C.; Robillard, B.; Jeandet, P. Kinetics of gas discharging in a glass of champagne: the role of nucleation sites. *Langmuir* **2002**, *18*, 1294−1301.
(5) Liger-Belair, G.; Marchal, R.; Jeandet, P. Close-up on bubble nucleation in a glass of champagne. *Am. J. Enol. Vitic.* **2002**, *53*, 151−153.
(6) Liger-Belair, G. The physics and chemistry behind the bubbling properties of champagne and sparkling wines: a state-of-the-art review. *J. Agric. Food Chem.* **2005**, *53*, 2788−2802.
(7) Voisin, C. Quelques aspects de la nucléation des bulles de champagne dans une flûte et de leur ascension à petits nombres de Reynolds, Ph.D. Thesis, Université de Reims Champagne-Ardenne, Reims, France, 2005.
(8) Ronteltap, A. D.; Hollemans, M.; Bisperink, C. G.; Prins, A. Beer foam physics. *Master Brew. Assoc. Am. Tech. Q.* **1991**, *28*, 25−32.
(9) Lynch, D. M.; Bamforth, C. W. Measurement and characterisation of bubble nucleation in beer. *J. Food Sci.* **2002**, *67*, 2696−2701.
(10) Liger-Belair, G.; Voisin, C.; Jeandet, P. Modeling non-classical heterogeneous bubble nucleation from cellulose fibers: application to bubbling in carbonated beverages. *J. Phys. Chem. B* **2005**, *109*, 14573−14580.
(11) Uzel, S.; Chappell, M. A.; Payne, S. J. Modeling the cycle of growth and detachment of bubbles in carbonated beverages. *J. Phys. Chem. B* **2006**, *110*, 7579−7586.
(12) Liger-Belair, G.; Tufaile, A.; Robillard, B.; Jeandet, P.; Sartorelli, J.-C. Period-adding route in sparkling bubbles. *Phys. Rev. E* **2005**, *72*, 037204.
(13) Packard, N. H.; Crutchfield, J. P.; Farmer, J. D.; Shaw, R. S. Geometry of a time series *Phys. Rev. Lett.* **1980**, *45*, 712−716.

Received for review May 4, 2006. Revised manuscript received July 24, 2006. Accepted July 26, 2006. Thanks are due to the Europôl'Agro institute and to the Association Recherche Oenologie Champagne Université for financial support.

JF061250N